

Molecular Dynamics Analysis of the Relation between the Spall Strength and Strain Rate for Solids

D. A. Indeitsev, A. M. Krivtsov, and P. V. Tkachev

Presented by Academician V.E. Fortov March 15, 2005

Received September 12, 2005

PACS numbers: 07.05.Tp, 46.15.-x, 62.20.-x

DOI: 10.1134/S1028335806030141

Experiments on the spall fracture of plates make it possible to investigate the strength properties of materials in a wide range of strain rates [1]. The characteristic feature of such experiments is the possibility of generating very high stresses in materials subjected to the simplest uniaxial deformation, which makes them irreplaceable in testing analytical and numerical models of the high-speed fracture of solids. A promising approach to simulating spall fracture is the use of the particle dynamics method (molecular dynamics) according to which a material is considered as a set of interacting particles (atoms) whose motion is described by classical dynamic equations. On the one hand, this discrete model allows the inclusion of the features of the behavior of a substance at the microlevel. On the other hand, this model with a large number of particles can be used to verify and test continuum medium models [2–7]. In classical molecular dynamics, particles are atoms, whereas in particle dynamics, they can also be associated with other structural elements (e.g., the grains of the material) or be used as specific finite elements, i.e., discrete carriers of the properties of the medium.

It is known that the spall strength of materials increases with the strain rate [1]. In this work, this effect is investigated using the particle dynamics method and the results are compared with the results of natural experiments [1]. Figure 1a shows the scheme of a computer experiment on the spall fracture. There are two rectangles filled with identical particles, striker and target (two-dimensional formulation of the problem is considered). The interaction between particles is described by the Lennard-Jones potential

$$\Pi(r) = D \left[\left(\frac{a}{r} \right)^{12} - 2 \left(\frac{a}{r} \right)^6 \right], \quad (1)$$

Institute of Problems of Mechanical Engineering, Russian Academy of Sciences, Vasil'evskii Ostrov, Bol'shoi pr. 61, St. Petersburg, 199178 Russia
e-mail: ind@director.ipme.ru, krivtsov@nm.ru, pavel_tkachev@mail.ru

where D is the binding energy and a is the equilibrium distance between particles. Particles form a close-packed triangular crystal lattice oriented so that one side of the triangles is parallel to the line separating the striker and target. The problem is numerically solved by integrating the equations of motion of particles:

$$M\ddot{\mathbf{r}}_k = \sum_{n=1}^N \frac{f(|\mathbf{r}_k - \mathbf{r}_n|)}{|\mathbf{r}_k - \mathbf{r}_n|} (\mathbf{r}_k - \mathbf{r}_n), \quad (2)$$

where \mathbf{r}_k is the radius vector of the k th particle, M is the particle mass, N is the total number of particles, and $f(r) \stackrel{\text{def}}{=} -\Pi'(r)$ is the interaction force between particles. At the initial time, particles forming the target are at rest and particles forming the striker move toward the target (the vertical direction in what follows) with a given velocity identical for all particles. The periodic and free boundary conditions are imposed in the horizontal and vertical directions, respectively. The simulation procedure was described in more detail in [6, 7].

If the velocity of the striker is high enough, as a result of the collision between two rarefaction waves reflected from the sample surfaces, a spall crack is formed in the target, which results in the separation of a fragment (spall plate) whose dimensions are approximately equal to those of the striker (Fig. 1b).

By varying the striker thickness, one can obtain impact pulses with various durations and correspondingly change the strain rate. In multiple computer experiments, the threshold striker velocity leading to a spall, i.e., spall velocity v_* , is determined for each thickness value. As the velocity scale, it is convenient to take the dissociation velocity

$$v_d \stackrel{\text{def}}{=} \sqrt{\frac{2D}{M}}, \quad (3)$$

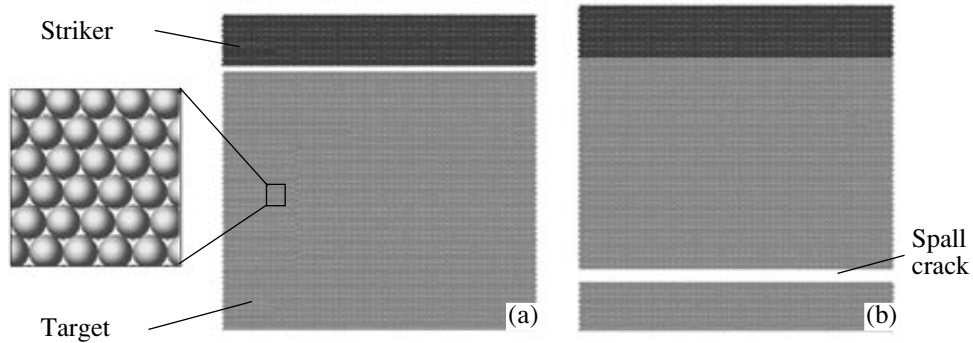


Fig. 1. Computer-experiment scheme: (a) the initial state of the sample and (b) the sample after spalling.

which is the minimum velocity necessary for a particle with mass M in equilibrium in potential field (1) to approach infinity.

Figure 2 shows the simulation results (calculations are performed for a sample containing 10^4 particles). The logarithm of the dimensionless spall velocity v_*/v_d as a function of the logarithm of the inverse striker thickness (N is the number of layers in the striker) is shown together with the corresponding trend line. The dependence obtained can be approximated by the relation

$$\frac{v_*}{v_d} = B \left(\frac{1}{N} \right)^m, \quad B = 1.7, \quad m = 0.16. \quad (4)$$

where B and m are the dimensionless constants.

Let us compare the results with the experimental dependences of the spall strength on the strain rate presented in [1]. Figure 3 shows the experimental dependences taken from Fig. 5.19 in [1] for titanium and

stainless steel. The strain rate $\dot{\epsilon} \stackrel{\text{def}}{=} \frac{\dot{V}}{V_0}$, where V is the specific volume of the medium, in the discharging part of the incident pulse is used as a quantity characterizing the time dependence of the spall strength σ_* . The axes show the common logarithms of the spall strength σ_* measured in gigapascals and strain rate $\dot{\epsilon}$ measured in inverse seconds. The experimental dependences can be approximated by the relation [1]

$$\sigma_* = A \left(\frac{\dot{V}}{V_0} \right)^m, \quad (5)$$

where A is a dimensional coefficient and m is a dimensionless exponent. The trend lines in Fig. 2 are plotted according to Eq. (5). In addition to the experimental dependences, the results of the computer experiment are also plotted in Fig. 2 under the assumption that the spall velocity v_* is proportional to the spall strength σ_*

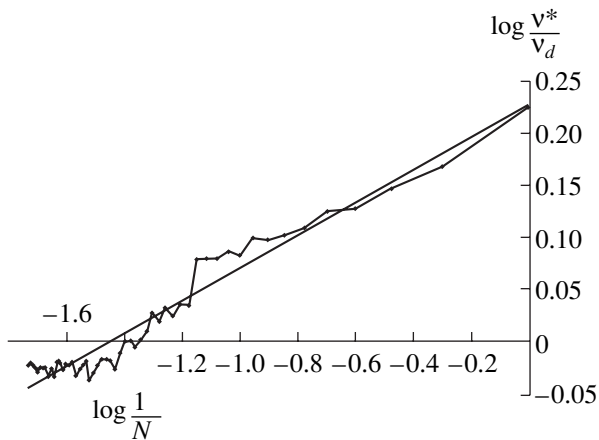


Fig. 2. Relative spall rate vs. inverse striker thickness (computer simulation).

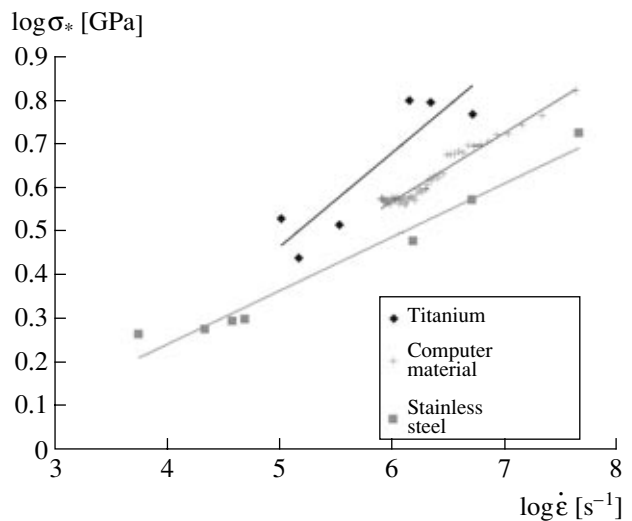


Fig. 3. Spall strength vs. strain rate according to the natural experiments [1] and computer simulation.

Exponent m in the dependence of the spall strength on the strain rate for various metals and computer material

Material	m
Titanium VT6	0.09
Stainless steel Kh18N10T	0.11
Lennard-Jones computer material	0.16
High-purity titanium	0.19
Copper	0.20
Aluminum AMg6M	0.21

and the inverse striker thickness $\frac{1}{N}$ is proportional to

the strain rate $\frac{\dot{V}}{V_0}$.¹ As a result, the results of the com-

puter experiment can be described by Eq. (5) and the exponent m must be the same in Eqs. (4) and (5). The table presents the exponents m for the computer and real materials [1]. As is seen, the m value for the computer material is between the values for stainless steel and high-purity titanium. We recall that Lennard-Jones potential (1) with only two parameters—the equilibrium distance a and binding energy D —is used for the computer material. The choice of these parameters ensures the horizontal and vertical shifts, respectively, of the strength–strain rate plot shown in Fig. 3 but does not affect the trend-line slope given by the exponent m , which is constant for the Lennard-Jones material.

Thus, the computer material considered under spall fracture exhibits properties close to the properties of real materials: the spall strength–strain rate plot is similar and its slope is between the values for stainless steel and high-purity titanium (see table). We note that these results are obtained for the simplest computer material,

¹ In order to determine the proportionality coefficients, the strain rate in the computer material was calculated at $a = 10^{-5}$ m (which corresponds to the approximate size of a grain for a number of metals) and the parameter D of Lennard-Jones potential (1) is chosen so that the A value for the computer material is equal to the average of the A values for titanium and stainless steel.

which is the close packing of particles interacting in accordance with the Lennard-Jones law. The close packing is more appropriate for single-crystal materials; however, according to the experiments, the difference between poly- and single-crystal materials is primarily in the dimensional coefficient A , whereas the exponent m in the dependence of the spall strength on the strain rate is almost identical for all these materials (see, e.g., Fig. 5.28 in [1]). The Lennard-Jones potential is classical for molecular dynamics and is usually used when considering the general properties of solids for the case where a qualitative description rather than a quantitative coincidence between the results is of primary interest. However, the above results show that it ensures satisfactory agreement with the experimental data. For more accurate calculations, one can use potentials with a larger number of parameters [8] that allow a better correlation with the properties of particular materials.

ACKNOWLEDGMENTS

We are grateful to N.F. Morozov for stimulating discussions. This work was supported by the Russian Foundation for Basic Research, project no. 05-01-00094.

REFERENCES

1. G. I. Kanel', S. V. Razorenov, A. V. Utkin, and V. E. Fortov, *Shock-Wave Phenomena in Condensed Media* (Yanus-K, Moscow, 1996) [in Russian].
2. B. L. Holian, *Shock Waves* **5** (3), 149 (1995).
3. F. F. Abraham, R. Walkup, H. Gao, et al., *Proc. Natl. Acad. Sci. USA* **99** (9), 5783 (2002).
4. A. M. Krivtsov, *Int. J. Impact Eng.* **23**, 477 (1999).
5. E. I. Golovneva, I. F. Golovnev, and V. M. Fomin, *Fiz. Mezomekh.* **6** (2), 39 (2003).
6. A. M. Krivtsov, *Fiz. Tverd. Tela* **46** (6), 64 (2004) [*Phys. Solid State* **46**, 1055 (2004)].
7. A. M. Krivtsov and V. P. Myasnikov, *Izv. Ross. Akad. Nauk, Mekh. Tverd. Tela*, No. 1, 87 (2005).
8. A. M. Krivtsov and N. V. Krivtsova, *Dal'nevostochnyĭ Mat. Zh.* **3** (2), 254 (2002).

Translated by R. Tyapaev